Talanta 195 (2019) 97–102

Contents lists available at ScienceDirect

Talanta

journal homepage: www.elsevier.com/locate/talanta

Naked eye detection of an amplified gene using metal particle-based DNA transport within functionalized porous interfaces

Yoo Min Park[a], Chi Hyun Kim[a], Younseong Song[a], Sang-Hyun Hwang[b], Seok Jae Lee[a], Moon-Keun Lee[a,*]

[a] Nano-Bio Application Team, National NanoFab Center (NNFC), 291 Daehak-ro, Yuseong-gu, Daejeon 34141, Republic of Korea
[b] Department of Laboratory Medicine, University of Ulsan, College of Medicine and Asan Medical Center, 88, Olympic-ro 43-gil, Songpa-gu, Seoul 05505, Republic of Korea

ARTICLE INFO

Keywords:
Naked eye detection of DNA
Point-of-care testing
Optical biosensor

ABSTRACT

The current study focuses on developing a system for visually detecting an amplified bacterial (*Escherichia coli* O157:H7) gene using a heavy metal particle (MP) and functionalized porous sepharose gel. To functionalize DNA-specificity to the MP, an avidin-modified MP was employed in combination with a biotin-conjugated primer. The porous sepharose matrix was functionalized with an amine-reactive group, such as N-hydroxysuccinimide (NHS), to achieve separation upon binding of the amplified gene. The pristine avidin-MPs strongly react with NHS-sepharose via imide bonds owing to the exposure of the amine group on the avidin-MP surface. Conversely, together with the amplified gene, the avidin-MPs are relatively less interactive toward the sepharose gel by steric hindrance of the amplified gene toward the imide bond between NHS and the amine groups. Owing to the higher molecular mass of the MP, those metal particles complexed with the amplified gene pass through the sepharose matrix when centrifugal force is applied. The MPs that are thus separated can be easily visualized by the naked eye owing to their inherent reddish-brown color. A polymerase chain reaction (PCR) product of *E. coli* O157:H7, present in concentrations ranging from 1.0×10^1 to 1.0×10^6 colony forming units (CFU), in actual food sample was evaluated with high sensitivity and reproducibility. We expect that the MP-based sensing system, which allows for visual detection of PCR-amplified genes, can be clinically used as a point-of-care testing device.

1. Introduction

Diagnostic technologies in the health care sector are consistently advancing and providing valuable point-of-care testing (POCT) devices on the field. Currently, novel biosensing principles have improved the availability of POCT devices for practical use by minimizing the procedure as well as reducing the biosensing apparatus [1–5]. Although high-technology based biosensing principles and equipment allow for highly reliable disease diagnosis [6], such instruments are mostly installed at clinical and laboratory facility levels owing to their requirements for high power sources, complex experimental methods and apparatus, and skilled experts for correct handling and completion of the entire process. Florescence and colorimetric principles related to target-specific light sources, filters, prisms, and visualization devices have been conventionally employed within the research and clinical fields of molecular diagnosis [7–12]. Furthermore, the techniques involve complex methodology and instrumentation requiring few experimental steps, relatively lengthy reaction times, or supplementary equipment for colorimetric development and detection. The high-tech biosensors are therefore usually inaccessible in molecular diagnosis to the general patients and users [13,14].

Several researchers have attempted to develop practically usable POCT devices in resource-limited settings based on the ASSURED criteria (affordable by those at risk of infection; sensitive, specific, user-friendly, rapid and robust, equipment-free, and delivered to those who need it) issued by the World Health Organization [15–18]. To meet the requirement of such cost competitiveness, minimization of biosensor, and user-friendliness in the commercial filed, we focused on developing a visually detectable molecular diagnostic technique involving simple colorimetry. Our diagnostic principle provides several merits, such as minimization of detection time, analytical devices, and power consumption. This simplified biosensing principle is based on visualization and was developed using a colored heavy metal particle (MP), e.g., magnetic beads. Magnetic beads contain heavy MPs having an inherent reddish-brown color. Magnetic beads have been conventionally used as a capture scaffold for separating and purifying various biomaterials, such as antibodies, antigens, whole cells, and nucleic acids, based on the simple principle of migration and surface modification [19–23]. Here we developed a MP-based visual detection principle, solely based on visualization with the naked eye, using functionalized sepharose with an amine-reactive group (e.g., N-

* Corresponding author.
E-mail address: mklee@nnfc.re.kr (M.-K. Lee).

https://doi.org/10.1016/j.talanta.2018.11.037
Received 12 October 2018; Received in revised form 12 November 2018; Accepted 12 November 2018
Available online 13 November 2018
0039-9140/

hydroxysuccinimide (NHS)) on the porous structure. A change in chromatographic distance can be easily visualized using an alteration of interaction between the MP and sepharose owing to DNA-involved steric hindrance. This chromatographic migration and visualization allowed us to avoid conventional equipment and procedures, such as gel electrophoresis, required for gene analysis. We verified the application of this system for detecting bacteria causing foodborne illnesses (*Escherichia coli* O157:H7). Using this biosensing platform, a gene amplified from *E. coli* O157:H7 isolated from an actual food sample using conventional PCR was evaluated by visualization with the naked eye without using any specific analytical device. Details of this biosensing principle are presented in this study.

2. Materials and methods

2.1. Materials and apparatus

N-Hydroxysuccinimidyl Sepharose® 4 Fast Flow (H8280) was obtained from Sigma Aldrich (St. Louis, USA). Dynabeads® Myone™ Streptavidin C1 (65001) was obtained from Invitrogen (MA, USA). Test tubes (AXY-MCT-060) were obtained from Axygen (NY, USA). HotStarTaq® Plus Master Mix kit (203643) was purchased from Qiagen (Hilden, Germany). Modified primer was synthesized and obtained from Bioneer (Daejeon, Korea). GelRed™ Nucleic Acid Gel stain 10,000 × (41,002) was obtained from Biotium (Hayward, CA, USA). Centrifuge (Combi-514R) was from Hanil Scientific (Gimpo-si, Korea). Dynamic Light Scattering (Zetasizer-Nano-ZS) was purchased from Malvern (Worcestershire, UK). The UV exposure unit (Slite 140) was obtained from AveGene (Taipei, Taiwan). QuickExtract™ DNA extraction solution 1.0 (QE09050) was purchased from Epicentre (WI, USA). PBS buffer (70013–032) was obtained from Gibco (MA, USA). The thermal cycler PCR System (C1000 Touch™, 184100) was obtained from Bio-Rad (CA, USA). Fluorometer (cytation3) was obtained from BioTek (Vermont, USA).

2.2. E. coli O157:H7 preparation and DNA extraction

E. coli O157:H7 was cultured for 16 h at 37 °C on *Luria-Bertani* medium. Colonies were counted using the colony counting method, and colony forming units (CFU) were estimated. Cells were harvested in test tubes by centrifugation at 2000 g force for 10 min, and bacterial DNA was extracted from the cell pellet using the QuickExtract™ DNA solution 1.0 at 98 °C for 15 min.

2.3. Polymerase chain reaction (PCR)

PCR was performed to validate the proof of concept of rapid visual identification of target DNA amplicons. Primer designs were based on *stx2* DNA [24]. The 5′ end of forward primers was labeled with biotin to react with streptavidin-conjugated magnetic beads. The sequence of the forward primer was 5′-GGGCAGTTATTTTGCTGTGGA-3′, whereas that of the reverse primer was 5′-TGTTGCCGTATTAACGAACCC-3′. PCR amplification was performed using the HotStarTaq® Plus Master Mix Kit containing 2X master mix, 0.08 μM each of forward and reverse primer, 1 μL extracted DNA, and deionized (DI) water. Thermal cycling conditions were as follows: 5 min at 95 °C; 35 cycles at 95 °C for 30 s, 60 °C for 30 s, 72 °C for 30 s; and 72 °C for 5 min. Target DNA was amplified using biotin-labeled forward primer for 120-bp sized amplicons.

2.4. Characterization of DNA flexibility and reactivity with GelRed

The hydrodynamic size of DNA with GelRed was measured using the dynamic light scattering (DLS) method to evaluate DNA flexibility based on its reaction with GelRed. A 100 nm streptavidin-modified MP was employed; the PCR product of 1.0×10^5 *E. coli* O157:H7 with or without GelRed was utilized, and 10-fold diluted GelRed was applied. The particle size of MP, MP/DNA, and MP/DNA/GelRed in the aqueous phase was sequentially measured.

Cross-reactivity of GelRed with the applied materials was also investigated. To this end, 1 μm streptavidin-modified MP, NHS-sepharose, and the *E. coli* O157:H7 PCR products were prepared. Each prepared sample was allowed to react with 10-fold diluted GelRed, and the sample mixtures were washed and resuspended in PBS buffer thrice. Fluorescence intensity and optical images of MP, MP/sepharose, and MP/sepharose/DNA were observed using a fluorometer and UV analyzer.

2.5. Optimization of GelRed concentration and centrifugation time

Various concentrations of GelRed were tested to effectively separate the MP. For this purpose, 150 μL NHS-sepharose was loaded in a test tube containing the following sample mixture: 1 μm MP (10 μL) and 10 μL PCR product. Following this, 1 μL of 5-, 10-, 50-, 100-, and 200-fold diluted GelRed was allowed to react with the sample mixtures for 20 min. Each test tube was subjected to centrifugation at 141 g force for 2 min and then observed. The centrifugation time was compared from 0 to 300 s at 141 g force using 1.0×10^1 and 1.0×10^5 CFUs of the *E. coli* O157:H7 PCR product. Each assay test tube was observed with the naked eye.

2.6. Manipulation of MP-bead column and visualization of amplified DNA

The principle of the rapid visual detection system is illustrated in Fig. 1. The final optimized protocol for this system included the following steps: after PCR amplification, a mixture of 10 μL biotinylated amplified DNA, 10 μL magnetic bead suspension (10 mg/mL), and 1 μL GelRed was pipetted into each sepharose-loaded test tube; The test tube was incubated for 5 min at 37 °C and then centrifuged at 141 g force for 2 min, following which a visual identification was performed by the naked eye. Reproducibility of the system was verified by 3X testing of *E. coli* O157:H7 in milk under identical conditions.

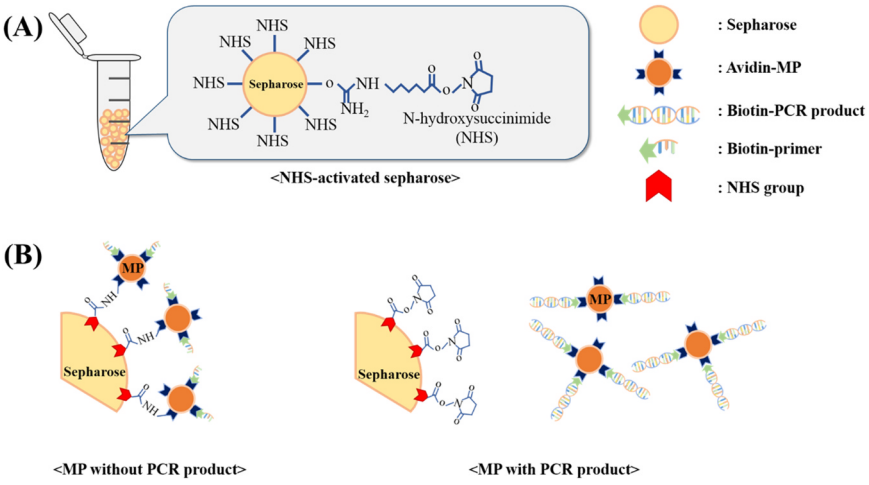

Fig. 1. Schematic illustration of MP-based PCR product separation principle. (A) The sepharose surface is modified with NHS group. (B) The pristine MP could be covalently reacted with sepharose, while the MP conjugated with DNA was isolated from sepharose surface by steric hindrance of double helical structure of PCR product.

3. Results and discussion

3.1. Biosensing principle of the MP-based naked eye analysis

Here, we developed a ligand affinity chromatography-based optical sensing platform, which does not require any complex analytical apparatus, for detecting PCR products with the naked eye. Streptavidin-conjugated MPs were used as the mobile phase and for transmitting a signal based on its inherent reddish-brown color. A biotin-conjugated primer was employed to directly bind to the MP and the PCR product. The use of NHS-functionalized sepharose as the stationary phase that captures the amine moiety enabled the separation of MPs according to their conjugation status with PCR products (Fig. 1 (A)). To establish the naked eye inspection principle, the target pathogen gene was initially amplified using conventional PCR and mixed with the prepared MPs, thereby changing the surface moieties on MPs according to their binding of biotin-labeled amplified gene to avidin (Fig. 1 (B)). This mixture was then gently loaded onto the top of sepharose-filled test tubes and centrifuged. The pristine MPs tended to remain on the upper layer of sepharose owing to covalent bonding of free avidin with NHS, whereas the MP–DNA complex was able to pass through the sepharose network owing to steric hindrance of DNA on the surface of the MP, thereby enabling observation of MP migration with the naked eye, without requiring any complex analytical device.

3.2. Feasibility study of the detection system

E. coli O157:H7 was selected as a pathogen biomarker for foodborne illnesses; a concentration of 1.0×10^5 CFU was used. The purified genomic DNA (gDNA) was sequentially mixed with MPs and diluted 10-fold using GelRed for 10 and 30 min, respectively. The mixtures were loaded onto test tubes filled with 200 µL NHS-modified sepharose (Fig. 2 (A)). To separate the MP, the test tubes were centrifuged at 141 g force for 2 min, and results were observed by the naked eye. Fig. 2 (B) clearly showed that the MP from the applied *E. coli* O157:H7 test migrated in the sepharose gel, whereas that from the negative control test with DI water did not. In the test conducted with DI water, the MP was found to be solidly bound with sepharose remaining as a thin layer on its surface. However, in case of *E. coli* O157:H7, the MP unconstrainedly passed through sepharose, indicating that it could evenly spread out within the poromeric network of sepharose. These results clearly indicate the feasibility of the proposed naked eye biosensing system for testing the presence of amplified pathogenic gene products.

3.3. Verification of DNA flexibility with GelRed

DNA flexibility is crucial to analytical efficiency because the amplified PCR product on the surface of the MP can sterically hinder the binding between the amine group of streptavidin and the NHS group on sepharose. Theoretically, it is well known that DNA strands exhibit high flexibility according to their base pair length in the aqueous phase [25,26]. For adjusting the DNA flexibility, GelRed was employed as a specific intercalator of double-stranded DNA. It has been reported that an intercalated double-stranded DNA complex exhibits relatively low flexibility in the aqueous phase owing to structural rigidity after intercalation [27,28]. We analyzed the hydrodynamic diameter of the MP–DNA complex by DLS to verify the DNA flexibility. Particle size variation was observed based on biomolecule dynamics. The 100-nm streptavidin-conjugated MPs were used to detect small changes in size. For this purpose, 1.0×10^5 CFU of *E. coli* O157:H7 were extracted and purified, following which the prepared gene was mixed with the PCR mixture containing the biotinylated primer. After PCR, the amplified gene was allowed to react with the MPs (100 nm), following which the GelRed (10-fold diluted) was mixed with the prior solution. As shown in Fig. 3 (A), the size of the pristine MPs was found to be 158 nm. Based on the size of the entire streptavidin moiety on the metal particle surface (20 nm) and the hydrodynamic size of the particle, the measured size of MPs was considered reliable [29]. The size of MP with DNA was found to be 191 nm. The size of the amplicons (100 bps) leads to a theoretical size of approximately 34 nm. Assuming that the amplified DNA uniformly binds with the surface of MP, the final expected increase in size should therefore be 68 nm. However, as previously mentioned, the length of DNA in the aqueous phase is variable; thus, the observed result proved the flexibility of the DNA. In the case of GelRed, the size of MP and DNA was measured to be 224 nm. This result supported the successful intercalation of GelRed and dsDNA, thereby allowing GelRed to decrease the flexibility of amplified DNA. Based on these findings, we could confirm that the reaction with GelRed was critical to adjust the flexibility of DNA in the biosensing system.

Because GelRed is exposed to various functional groups on MPs and sepharose, a nonspecific binding (NSB) of GelRed may induce an unexpected signal. To verify the reactivity of GelRed, its fluorescent property was utilized and UV radiation was used to detect fluorescence. Further, to compare the binding affinity of GelRed, three samples were prepared in tubes: sepharose, sepharose with MP, and sepharose with MP and PCR product. GelRed (10-fold diluted) was loaded onto each of the prepared tubes and was allowed to react for 10 min. The resuspended solution was repeatedly spun down in PBS buffer, and fluorescence was observed under UV radiation (Fig. 3 (B)). As shown in the inset of Fig. 3 B, fluorescence was observed in the samples containing sepharose/MP/DNA, whereas samples containing only sepharose and sepharose/MP showed no fluorescence signals, thereby indicating a specific intercalation of GelRed with double-stranded DNA without cross-reactivity with either sepharose or MP. For an accurate optical analysis, the fluorescence intensity of identical samples was also measured using a fluorometer. The

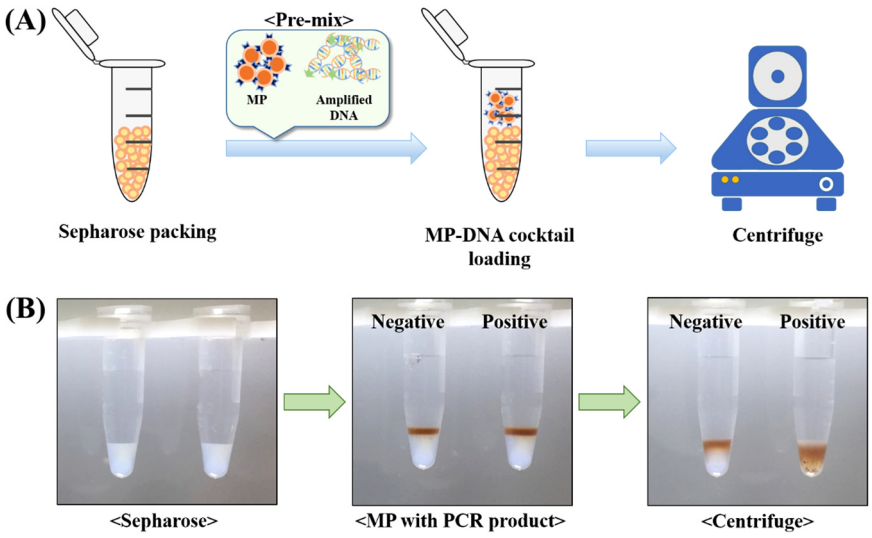

Fig. 2. (A) An illustration of the MP-based naked eye detection of PCR product. The MP on the sepharose was simply separated by centrifuge. (B) The feasibility test of developed biosensing system using the 1.0×10^5 CUF of *E. coli* O157:H7. The MP on the sepharose was selectively migrated in accordance with PCR product.

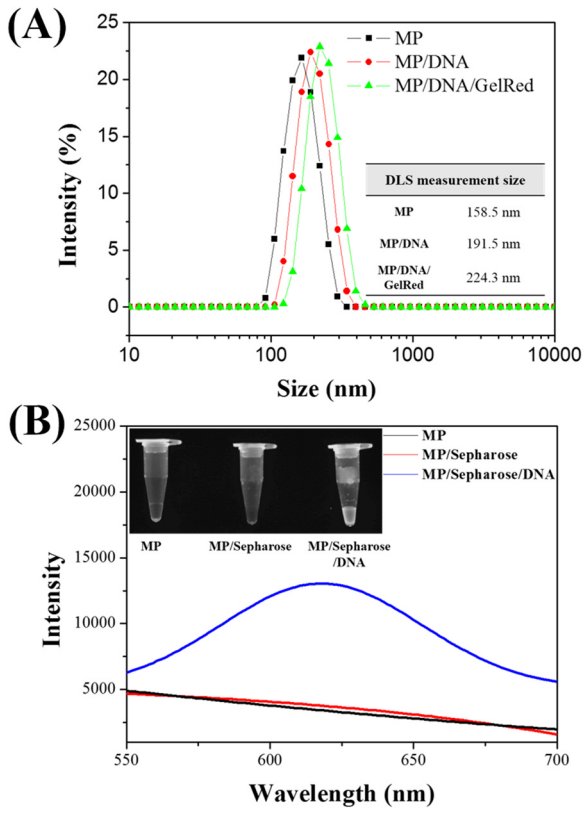

Fig. 3. (A) Verification of DNA flexibility associated with intercalator by DLS method. The hydrodynamic of MP, MP/DNA, and MP/DNA/GelRed was sequentially observed. (B) The cross-reactivity test of GelRed to the MP, sepharose, and DNA. The GelRed was reacted with the prepared materials, and the GelRed reactivity was confirmed by fluorometry.

optical signal was scanned from 550 to 700 nm because the maximum emission wavelength was 620 nm. Fig. 3 (B) shows an intense fluorescent signal in the sepharose/MP/DNA sample; however, no signal was detected in the samples containing sepharose and sepharose/MP. Together, these results reveal the expected functionality of GelRed in the naked eye detection system.

3.4. Optimization of GelRed concentration and reaction time

GelRed was selected as the DNA intercalator of choice and was optimized based on previous reliable testing (Fig. 3 (A)). The GelRed concentration needed to be optimized because the functionality of GelRed is related to the binding affinity between MP with sepharose. The migration of MP after subjecting to relevant GelRed concentration gradient (refer Materials and Methods, Section 2.5) and subsequent centrifugation was observed as shown in Fig. 4 (A). Aggregated MP could be detected on the sepharose gel in the sample containing 5-fold diluted GelRed. We assume that a high concentration of GelRed may have led to its self-aggregation and may have increased the reaction of MP with sepharose, thereby affecting the migration of MP. In the sample containing 10-fold GelRed, the MP was observed to migrate in the sepharose gel. This change was not observed in the sample containing no PCR product. A change in the MP layer was also observed in samples containing 50-, 100-, and 200-fold diluted GelRed. Most of the MP was retained on the upper part of sepharose, thereby indicating the inefficiency to distinguish variation in signals. In samples that did not contain GelRed, the MP was only slightly changed because of the low binding affinity of MP with sepharose. In the samples that did not contain the PCR product, the position of the MP layer was observed to be similar to that of the initial state. This finding supported the assumption that GelRed was not involved in the reaction of MP with sepharose. Based on these results, a 10-fold dilution of GelRed was considered optimal for precisely evaluating results, and this optimized condition was employed in all further tests.

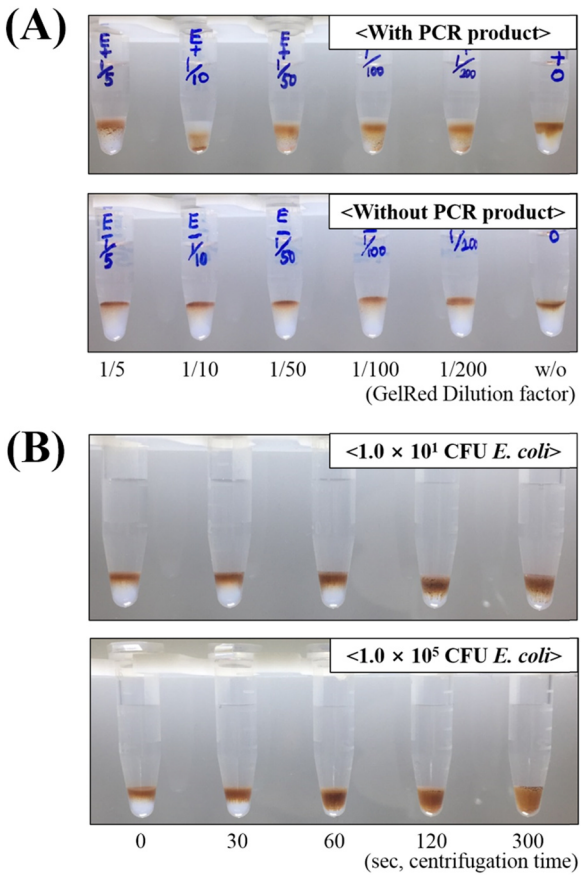

Fig. 4. Optimization of intercalator concentration and centrifugation time. (A) The GelRed concentration was serially diluted and applied to the MP-based optical sensor. The 1/10 diluted GelRed was selected as the optimized concentration. (B) The centrifugation time was optimized using the 1.0×10^1 and 1.0×10^5 CFU of *E. coli* O157:H7. The 120 s was optimized to observe the MP separation by naked eye.

Furthermore, the centrifugation time was also optimized to obtain the best possible results. Samples containing 1.0×10^1 and 1.0×10^5 CFU of *E. coli* O157:H7 were tested. Each test tube containing the relevant bacterial sample was centrifuged at 141 g force for 0, 30, 60, 120, and 300 s. As shown in Fig. 4 (B), the migration pattern of MP in the samples containing 1.0×10^1 CFU *E. coli* O157:H7 changed sequentially upon centrifugation from 0 to 120 s, and the MP level was observed to saturate at 120 s. Here, the MPs were observed to move and stabilize at the center of the test tube, thus suggesting a low concentration of the amplified gene. In samples containing 1.0×10^5 CFU of *E. coli* O157:H7, the MP layer was observed to be gradually altered as the centrifugation time increased from 0 to 60 s. MPs were located at the bottom of the test tube and could be observed with the naked eye. Although a centrifugation time of 60 s was enough to completely pellet down a high concentration of *E. coli* O157:H7, a centrifugation time of 120 s was selected to effectively analyze the various concentrations of *E. coli* O157:H7. Based on these findings, we could successfully demonstrate that the MPs could be effectively separated using the optimum centrifugation time of 120 s and by applying a 10-fold dilution of GelRed.

3.5. Verification of sensitivity limit for E. coli O157:H7 analysis

A minor amount of *E. coli* O157:H7 in food may cause foodborne illnesses. Hence, it was necessary to establish the sensitivity of the developed biosensing principle. To confirm the limit of detection (LOD) of *E. coli* O157:H7, the concentration detection of the lowest amount of the bacterium in a single reaction was evaluated. *E. coli* O157:H7 culture was sequentially diluted from 1.0×10^6 to 1.0×10^1 CFU, and the target

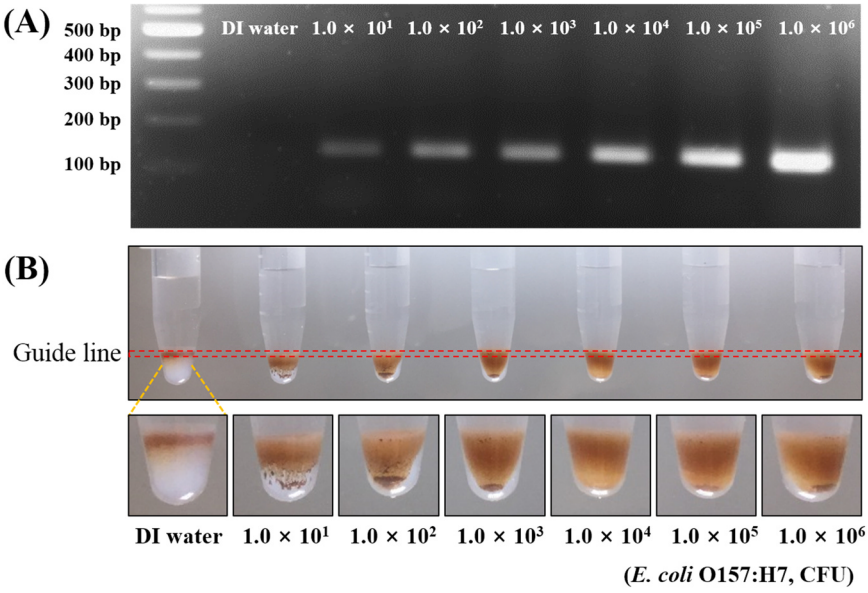

Fig. 5. (A) The test result of PCR product of *E. coli* O157:H7 from 1.0×10^1 to 1.0×10^6 CFU using the gel electrophoresis. (B) The MP-based *E. coli* O157:H7 test result. The MP from the whole *E. coli* O157:H7 concentration was separated, while, in the negative control, the MP was detected on the sepharose surface. The MP migration is able to be observed by naked eye. The guide line is presented on the images to clearly analyze the MP changes.

gene was amplified using conventional PCR from lysed and purified cells. Each PCR product was evaluated using the developed biosensing platform under optimized test conditions. As shown in Fig. 5 (A), the presence of PCR products could be confirmed using poly-acrylamide gel electrophoresis; the obtained optical image corresponded with the concentration of the amplified gene. Using identical samples, the MP-based sensing platform could be implemented. Fig. 5 (B) shows a red dotted line as a guide for clearly distinguishing the change of MP position, as observed by the naked eye. In the magnified result images, migration of MP was obvious within the entire test-range of *E. coli* O157:H7 concentration i.e., from 1.0×10^1 to 1.0×10^6 CFUs, and not in the negative control sample. The position of the MP layer was accurately distinguishable from that in the negative control solely by visual detection despite the fact that the MP migrated only slightly in samples containing 1.0×10^1 CUF of *E. coli* O157:H7. Thus, the limit of *E. coli* O157:H7 detection in the MP-based biosensor was observed to be as low as 1.0×10^1 CFU. Hence, we could confirm that this optical biosensor can very sensitively identify pathogenic *E. coli* O157:H7 by visual detection via the naked eye without requiring any specific analytical equipment, such as fluorescent, luminescent, or image measurement devices.

3.6. Visual analysis and naked eye detection of E. coli O157:H7 in milk

Because *E. coli* O157:H7 is one of the primary causes of foodborne illnesses, it was analyzed and detected in actual food samples to verify the applicability of this principle of detection. A 10-μL milk sample was spiked by artificially infecting it with serial dilutions (1.0×10^6 to 1.0×10^1 CFUs) of *E. coli* O157:H7. DNA was isolated from these artificially infected milk samples, and subsequent PCR was performed. The PCR products were then loaded onto the MP-based biosensor developed

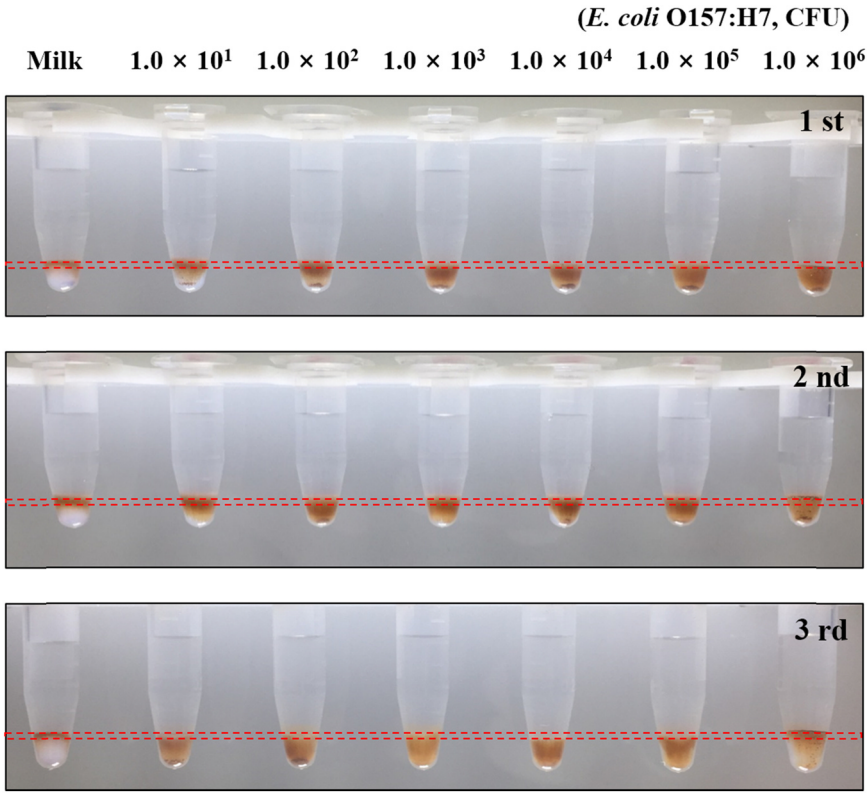

Fig. 6. Milk-based *E. coli* O157:H7 from 1.0×10^1 to 1.0×10^6 CUF evaluation. The PCR product from the milk-spiked *E. coli* O157:H7 was applied to the MP-based optical biosensor, and the migrated MP was observed in the whole *E. coli* O157:H7 concentration, while the MP stays on the sepharose in the milk test. The same test was conducted under same condition such pH, reaction time, and temperature, and all test results were significantly similar, indicating high reproducibility.

in this study. The detection of *E. coli* O157:H7 was repeated under identical experimental conditions mentioned in this study (temperature, concentration, and reaction time), and the reproducibility and reliability of the results is presented in Fig. 6. The images of the MP layer of the applied *E. coli* O157:H7 were obtained, and the MP was clearly migrated in the entire detection range. To accurately observe the MP levels, the guidelines for determination were presented as a red dotted line in the result images. In the result from 1.0×10^1 CFU *E. coli*, the MP was immigrated at the middle of tube, whereas the signal variation between negative and positive was distinguishable; thus, we verified that the real food-based *E. coli* O157:H7 was successfully evaluated by employing the naked eye-based optical biosensing system without requiring any specific analytic devices. The LOD of the developed system was 1.0×10^1 CFU *E. coli* O157:H7 in the real sample, indicating the high sensitivity. Consequently, the same sample was repeatedly implemented, and the second and third test results are presented in Fig. 6 (middle and bottom). The negative control from the second set was slightly changed, whereas the signal variation was distinguishable with PCR product test. We assumed that the MP could be partially passed though the weak network on the functional structure of the sepharose gel. The MP in the positive control samples was certainly migrated, and these test results were similar to those of the first result, thus indicating high reproducibility.

Conventionally, electrophoresis is the method that is commonly employed in laboratories or in the clinical detection of PCR products. Although electrophoresis leads to highly accurate and reproducible results, it needs a long test-time of approximately 1 h, including a complex sample preparation procedure. Contrarily, the principle of PCR product detection developed in this study could accurately evaluate the presence of the amplified target gene within 2 min. Because the results obtained in this study were reliable and reproducible, our novel optical analysis principle can be effectively employed as an on-site quality inspection tool.

4. Conclusion

This study exhibited the successful development and application of a PCR-amplified fragment detection system, detectable with the naked eye, that utilizes the migration of MPs within a functionalized network structure of sepharose gel. Based on the modification of the colorimetric properties of heavy metals using simple surface engineering, PCR products could easily be observed visually by the naked human eye, without requiring any sophisticated technical devices. This novel biosensing system will successfully reduce the cost and time spent in detecting genes from the pathogenic strain of *E. coli* O157:H7 in food products to as little as less than 2 min. Further, this novel system demonstrated a high level of reproducibility and sensitivity and could detect PCR products in samples containing as concentrations of bacteria as low as 10×10^1 CFUs. This novel MP-based biosensor system may pave the way further commercial opportunities because metal particles are widely employed in several commercial biochemical assays. The reliable and encouraging results from this study exhibit an outstanding potential for developing the current optical biosensing platform as a POCT device and a useful tool for PCR product assessment.

Acknowledgment

This work was supported by Nano Material Technology Development Program through the National Research Foundation of Korea (NRF) funded by the Ministry of Science and ICT (No. 2017M3A7B4039936), and the National Research Foundation of Korea (NRF) Grant funded by the Korean Government (MSIP) (No. 2014R1A5A2010008). Also this work was supported by Cooperative Research Program for Agriculture Science & Technology Development (Project No. PJ01252602) from the Rural Development Administration (RDA) of the Republic of Korea.

References

[1] Y.M. Park, S.J. Kim, K.J. Lee, S.S. Yang, B.-H. Min, H.C. Yoon, Detection of CTX-II in serum and urine to diagnose osteoarthritis by using a fluoro-microbeads guiding chip, Biosens. Bioelectron. 67 (2015) 192–199.
[2] Y.T. Kim, D. Lee, H.Y. Heo, J.E. Sim, K.M. Woo, D.H. Kim, S.G. Im, T.S. Seo, Total integrated slidable and valveless solid phase extraction–polymerase chain reaction–capillary electrophoresis microdevice for mini Y chromosomes short tandem repeat genotyping, Biosens. Bioelectron. 78 (2016) 489–496.
[3] Y.M. Park, Y.D. Han, H.J. Chun, H.C. Yoon, Ambient light-based optical biosensing platform with smartphone-embeded illumination sensor, Biosens. Bioelectron. 93 (2017) 205–211.
[4] Y.M. Park, S.Y. Lim, S.J. Shin, C.H. Kim, S.W. Jeong, S.Y. Shin, N.H. Bae, S.J. Lee, J. Na, G.Y. Jung, T.J. Lee, A film-based integrated chip for gene amplification and electrochemical detection of pathogens causing foodborne illnesses, Anal. Chim. Acta 1027 (2018) 57–66.
[5] R.-J. Yang, L.-M. Fub, H.-H. Hou, Review and perspectives on microfluidic flow cytometers, Sens. Actuators B 266 (2018) 26–45.
[6] P.W. Uys, R. Warren, P.D. van Helden, M. Murray, T.C. Victor, Potential of rapid diagnosis for controlling drug-susceptible and drug-resistant tuberculosis in communities where *Mycobacterium tuberculosis* infections are highly prevalent, J. Clin. Microbiol. 47 (2009) 1484–1490.
[7] C.D. Ahrberg, A. Manz, P. Neuzil, Single fluorescence channel-based multiplex detection of avian influenza virus by quantitative PCR with intercalating dye, Sci. Rep. 5 (2015) 11479.
[8] G.G. Morbioli, T. Mazzu-Nascimento, A.M. Stockton, E. Carrilho, Technical aspects and challenges of colorimetric detection with microfluidic paper-based analytical devices – a review, Anal. Chim. Acta 970 (2017) 1–22.
[9] J. Huang, X.-Y. Li, Y.-C. Du, L.-N. Zhang, K.-K. Liu, L.-N. Zhu, D.-M. Kong, Sensitive fluorescent detection of DNA methyltransferase using nicking endonuclease-mediated multiple primers-like rolling circle amplificaiton, Biosens. Bioelectron. 91 (2017) 417–423.
[10] J. Kudr, L. Richtera, K. Xhaxhiu, D. Hynek, Z. Heger, O. Zitka, V. Adam, Carbon dots based FRET for the detection of DNA damage, Biosens. Bioelectron. 92 (2017) 133–139.
[11] H.-S. Yin, B.-C. Li, Y.-L. Zhou, H.-Y. Wang, M.-H. Wang, S.-Y. Ai, Signal-on fluorescence biosensor for microRNA-21 detection based on DNA strand displacment reation and Mg^{2+}-dependent DNAzyme cleavage, Biosens. Bioelectron. 96 (2017) 106–112.
[12] L. Xue, L. Zheng, H. Zhang, X. Jin, J. Lin, An ultrasensitive fluorescent biosensor using high gradient magneticseparation and quantum dots for fast detection of foodbornepathogenic bacteria, Sens. Actuators B 265 (2018) 318–325.
[13] D. Mabey, R.W. Peeling, A. Ustianowski, M.D. Perkins, Diagnostics for the developing world, Nat. Rev. Microbiol. 2 (2004) 231–240.
[14] R.W. Peeling, D. Mabey, Point-of- care tests for diagnosing infections in the developing world, Clin. Microbiol. Infect. 16 (2010) 1062–1069.
[15] C.D. Chin, V. Linder, S.K. Sia, Commercialization of microfluidic point-of-care diagnostic devices, Lab Chip 12 (2012) 2118–2134.
[16] A.K. Yetisen, M.S. Akram, C.R. Lowe, Paper-based microfluidic point-of-care diagnostic devices, Lab Chip 13 (2013) 2210–2251.
[17] P.K. Drain, E.P. Hyle, F. Noubary, K.A. Freedberg, D. Wilson, W.R. Bishai, W. Rodriguez, I.V. Bassett, Diagnostic point-of-care tests in resource-limited settings, Lancet Infect. Dis. 14 (2014) 239–249.
[18] W.K.T. Coltro, C.-M. Cheng, E. Carrilho, D.P. de Jesus, Recent advances in low-cost microfluidic platform for diagnostic applications, Electrophoresis 35 (2014) 2309–2324.
[19] M. Ben Ismail, E. de la Serna, G. Ruiz-Vega, T. García-Berrocoso, J. Montaner, M. Zourob, A. Othmane, E. Baldrich, Using magnetic beads and signal amplifiers to produce short and simple immunoassays: application to MMP-9 detection in plasma samples, Anal. Chim. Acta 999 (2018) 144–154.
[20] S. Bi, Z. Zhang, Y. Dong, Z. Wang, Chemiluminescence resonance energy transfer imaging on magnetic particles for single-nucleotide polymorphism detection based on liagtion chain reaction, Biosens. Bioelectron. 65 (2015) 139–144.
[21] J.A. DuVall, S.T. Cabaniss, M.L. Angotti, J.H. Moore, M. Abhyankar, N. Shukla, D.L. Mills, B.G. Kessel, G.T. Garner, N.S. Swami, J.P. Landers, Rapid detection of *Clostridium difficile via* magnetic bead aggregation in cost-effective polyester microdevices with cell phone image analysis, Analyst 141 (2016) 5637–5645.
[22] S.-H. Hwang, D.-E. Kim, J.-H. Im, S.-J. Kang, D.-H. Lee, S.J. Son, Rapid visual identification of PCR amplified nucleic acids by centrifugal gel separation: potential use for molecular point-of-care tests, Biosens. Bioelectron. 79 (2016) 829–834.
[23] C.-B. Kim, E.-G. Lim, S.W. Shin, H.J. Krause, H. Hong, Magnetic immunoassay platform based on the planar frequency mixing magnetic technique, Biosens. Bioelectron. 83 (2016) 293–299.
[24] V.K. Sharma, E.A. Dean-Nystrom, T.A. Casey, Semi-automated fluorogenic PCR assays (TaqMan) for rapid detection of *Escherichia coli* O157:H7 and other Shiga toxigenic *E.coli*, Mol. Cell. Probes 13 (1999) 291–302.
[25] J.D. Kahn, E. Yun, D.M. Crothers, Detection of localized DNA flexibility, Nature 368 (1994) 163–166.
[26] A.K. Mazur, M. Maaloum, DNA flexibility on short length scales probed by atomic force microscopy, Phys. Rev. Lett. 112 (2014) 068104.
[27] A. Jaffé-Brachet, J.M. Ruysschaert, The flexibility of a complex of DNA with methylated proflavine, Biochim. Biophys. Acta 224 (1970) 654–656.
[28] F. Jia, S. Despax, J.-P. Münch, P. Hébraud, Flexibility of short ds-DNA intercalated by a dipyridophenazine ligand, Front. Chem. 3 (2015) 25.
[29] S. Zhang, Y. Zhao, Facile synthesis of multivalent water-soluble organic nanoparticles via “surface clicking” of alkynylated surfactant micelles, Macromolecules 43 (2010) 4020–4022.